Published by Institute of Physics Publishing for SISSA

Received: *June 24, 2008*
Accepted: *July 10, 2008*
Published: *July 22, 2008*

Topological entanglement entropy and holography

Ari Pakman and Andrei Parnachev

C.N. Yang Institute for Theoretical Physics, Stony Brook University,
Stony Brook, NY 11794-3840, U.S.A.
E-mail: pakman@insti.physics.sunysb.edu, andreipv@insti.physics.sunysb.edu

Abstract: We study the entanglement entropy in confining theories with gravity duals using the holographic prescription of Ryu and Takayanagi. The entanglement entropy between a region and its complement is proportional to the minimal area of a bulk hypersurface ending on their border. We consider a disk in 2+1 dimensions and a ball in 3+1 dimensions and find in both cases two types of bulk hypersurfaces with different topology, similar to the case of the slab geometry considered by Klebanov, Kutasov and Murugan. Depending on the value of the radius, one or the other type of hypersurfaces dominates the calculation of entanglement entropy. In 2+1 dimensions a useful measure of topological order of the ground state is the topological entanglement entropy, which is defined to be the constant term in the entanglement entropy of a disk in the limit of large radius. We compute this quantity and find that it vanishes for confining gauge theory, in accord with our expectations. In 3+1 dimensions the analogous quantity is shown to be generically nonzero and cutoff-dependent.

Keywords: AdS-CFT Correspondence, Confinement, Field Theories in Lower Dimensions.

JHEP07(2008)097

Contents

1. Introduction and summary **1**

2. Review of the background material **3**
- 2.1 Entanglement entropy and the holographic prescription 3
- 2.2 Measures of quantum order and topological entanglement entropy 4

3. D3 branes on a circle **5**
- 3.1 Conformal limit 5
- 3.2 Finite compactification radius 8

4. D4 branes on a circle **11**
- 4.1 The two topologies 13
- 4.2 The phase transition 14
- 4.3 Topological entropy 15

5. Discussion **17**

A. Solutions in detail **18**

JHEP07(2008)097

1. Introduction and summary

Certain systems in two spacial dimensions are known to exhibit topological order [1, 2]. In this case the ground state of the system has highly non-trivial properties, related to the degeneracy on higher genus surfaces and the existence of quasi-particle excitations. Such a non-local order can exist even when local order parameters vanish. Recently a quantity called "topological entanglement entropy" was proposed [3, 4] to measure the degree of topological entanglement. It involves computing the entanglement entropy of a large disk and extracting the constant term, which does not scale with the circumference of the disk. The natural generalization to higher dimensions would involve entanglement entropy of a large ball.

Computing the entanglement entropy for a general system is not a trivial exercise. Recently Ryu and Takayanagi [5] proposed a way to compute the entanglement entropy in theories with holographic dual. The computation involves finding a certain minimal surface in the bulk of the asymptotically AdS space.[1]

[1] Schwimmer and Theisen [6] argued that anomalous terms in the entanglement entropy are not correctly reproduced in the holographic prescription. However the validity of this claim has been questioned in [7]. The strong subadditivity of the holographic entanglement entropy has been studied in [8, 9]. Covariant proposal for computing entanglement entropy was formulated in [10]. In [11] entanglement entropy in Little String Theory has been studied. Other interesting work includes [12, 13]–[14].

This hypersurface approaches the border between the region and its complement on the boundary. The generalization of this prescription also exists for the theories whose duals are not asymptotically AdS. In this paper we make use of this proposal to compute the topological entanglement entropy of some simple confining theories in 2+1 and 3+1 dimensions.

More precisely, we will study D3 and D4 branes compactified on a circle, which at large distances become confining 2+1 and 3+1 dimensional theories respectively. The entanglement entropy of the "slab" (the subspace defined by $-\ell/2 < x < \ell/2$, where x is one of the spacial coordinates) in these systems has been studied in [15]. As it turns out, there are two types of minimal surfaces: connected and disconnected ones. In ref. [15] a first order phase transition between these two types of solutions was observed as a function of ℓ. For small ℓ the connected solution dominates the computation of entanglement entropy, while for large ℓ the disconnected solution becomes preferred. The authors interpreted this phase transition as a signature of confinement. In the case of a disk in 2+1 dimensions or a ball in 3+1 dimensions there is again a single parameter R, and as we will see below there are again two types of solutions in the bulk. The analog of a connected solution has a disk topology and dominates at smaller values of R. In this solution the circle (sphere) which is the boundary of the disk (ball) shrinks to zero size in the bulk, while Kaluza-Klein circle remains finite. The analog of the disconnected solution has a cylinder topology and dominates at larger values of R. This is the solution where the Kaluza-Klein circle shrinks to zero size. For intermediate values of R the structure has a classic "swallowtail" shape typical of first order phase transitions.

To compute the topological entanglement entropy in 2+1 dimensions, we need to consider a disk whose radius is very large compared to the correlation length. In this regime the only available solution has the topology of a cylinder. We show that this solution approaches the straight cylinder as $R\to\infty$, and the topological entropy associated to it vanishes. In hindsight, this is not very surprising, since we do not expect long-range topological order in the ground state of $2+1$ dimensional QCD. Our calculation hence can be viewed as a consistency check on both the holographic prescription for computing entanglement entropy and topological entanglement entropy. Note that the existence of phase transition between the two topologies is crucial for the whole picture to be consistent.

We then compute the entanglement entropy in the theory on $D4$ branes compactified on a circle (this theory has many features of QCD in 3+1 dimensions, as emphasized in [16]). The structure of the solutions is similar to the 2+1 dimensional case. There is again a first order phase transition between the hypersurfaces of disk and cylinder topology, as R is varied. However when computing the radius-independent term we encounter a surprise: it contains an explicit dependence on the cutoff. We attribute this to the unconventional UV properties of the theory (see discussion section).

The rest of the paper is organized as follows. In the next section we review the definitions of entanglement and topological entanglement entropies and the holographic proposal of Ryu and Takayanagi. In section 3 we start with a warm-up example of a cylinder in $\mathcal{N}=4$ super Yang Mills in 3+1 dimensions and investigate the structure of the solutions. We then compactify the theory on a circle to generate a confining theory in

JHEP07(2008)097

$2+1$ dimensions. We re-investigate the structure of the solutions, compute the value of entanglement entropy as a function of R and extract the value of topological entanglement entropy, which vanishes. In section 4 we repeat this analysis for the case of the $D4$ branes compactified on a circle. We find a very similar phase transition structure, while the generalization of topological entanglement entropy turns out to be cutoff-dependent. We discuss our results in section 4. Appendix contains some details regarding the structure of the minimal hypersurfaces.

2. Review of the background material

2.1 Entanglement entropy and the holographic prescription

Consider a pure quantum state $|\Psi\rangle$ in a system that can be subdivided into two subsystems A and B. If we trace its density matrix over the degrees of freedom of B,

$$\rho_A = Tr_B \left(|\Psi\rangle\langle\Psi| \right) , \tag{2.1}$$

the density matrix ρ_A will be in general in a mixed state. Its von Neumann entropy

$$S_A = -Tr_A \left(\rho_A \ln \rho_A \right) \tag{2.2}$$

is called the *entanglement entropy* and is a measure of the entanglement between A and B in the original state $|\Psi\rangle$. In particular, it is zero if $|\Psi\rangle$ is the product of a state in A and a state in B, and one can verify that $S_A = S_B$.

Of particular interest is the case when the two subsystems A and B correspond to two regions in the spacetime of a local quantum field theory and $|\Psi\rangle$ is the ground state [17, 18]. In this case the entanglement entropy is cutoff dependent and its leading term is proportional to the area of the surface that separates the two regions.

For quantum field theories which have gravitational duals [19], the authors of [5] proposed a simple geometric prescription for computing the entanglement entropy of the vacuum. For a $d+1$ dimensional conformal field theory with an AdS_{d+2} dual, the idea is to find a d-dimensional surface Γ which minimizes the action

$$S_A = \frac{1}{4G_N^{(d+2)}} \int_\Gamma d^d\sigma \sqrt{G^{(d)}_{\rm ind}} \tag{2.3}$$

and approaches the boundary of the regions A and B at the boundary of the AdS_{d+2} manifold. The surface Γ is defined at a fixed time and $G^{(d)}_{\rm ind}$ is the induced string frame metric. As shown in [5], for the case of AdS_3, this prescription reproduces precisely the known expression for the entaglement entropy in 2D CFT, and has been subjected to several tests.

When the boundary theory is not conformal, which is the case we will be interested in this work, the above functional generalizes to

$$S_A = \frac{1}{4G_N^{(10)}} \int_\Gamma d^8\sigma e^{-2\phi} \sqrt{G^{(8)}_{\rm ind}} \tag{2.4}$$

where now Γ extends in all remaining directions.

JHEP07(2008)097

2.2 Measures of quantum order and topological entanglement entropy

Following the discovery of the Fractional Quantum Hall states [20], it became clear that there are quantum systems in which different phases or orders (e.g. quantum Hall states with different filling fractions) preserve the same symmetries. At zero temperature, different orders have different quantum correlations between the microscopic degrees of freedom, but cannot be distinguished by any local order parameter. For these *quantum orders*, Landau's theory of symmetry-breaking and local order parameter is inadequate, and novel quantum numbers are needed to characterize them.

When the system has an energy gap the quantum order is called *topological order* [21], and the theory is described in the infrared by a topological quantum field theory. Useful characterizations of topological orders are the degeneracy (in the infinite volume limit) of the ground state in a Riemann surface as a function of the genus [22, 1], the spectrum of quasiparticle excitations [23] and the structure of the gapless edge excitations [2].

Another quantum number which characterizes topological order is the total quantum dimension, defined as follows. The number of linearly-independent states having N quasiparticles of type a, for large N, is proportional to d_a^N, where d_a is the quantum dimension of the quasiparticle a [24]. The *total quantum dimension* of the system is

$$\mathcal{D} = \sqrt{\sum_a d_a^2}\,. \tag{2.5}$$

In general, $\mathcal{D} > 1$ signals a topological order. In theories with no quasiparticle excitations, as in the model we consider in the next section, only the identity sector contributes to (2.5), so we expect $\mathcal{D} = d_I = 1$.

As it turns out, the total quantum dimension $\mathcal{D}$ is intimately related to the entanglement properties of the ground state. Consider, in $2+1$ dimensions, a disk A with a smooth boundary of length L in the infinite plane. It was shown in [3, 4] that the entanglement entropy of the ground state between the disk A and its exterior behaves as

$$S_A = \alpha L - \log \mathcal{D} + \cdots \tag{2.6}$$

where α is non-universal and cutoff dependent and the additional terms vanish in the limit $L \to \infty$. The quantity

$$\gamma = \log \mathcal{D} \tag{2.7}$$

is called *topological entanglement entropy*. It is a measure of topological order encoded in the wave-function, and not in the spectral properties of the Hamiltonian, as the other characterizations of topological order mentioned above. For theories in $2+1$ dimensions whose boundary degrees of freedom live in a 2D conformal field theory, the topological entanglement entropy can be expressed in terms of the modular matrix of the latter. For studies exploiting this idea see [25, 26].

The definition of γ can be naturally generalized to dimensions higher than $2+1$ by considering a ball instead of a disk, but these cases have not been thoroughly studied yet.[2]

[2]Solvable systems exhibiting topological order in $3+1$ dimensions were studied in [27].

3. D3 branes on a circle

Here we consider entanglement entropy for a disk in the strongly coupled four-dimensional $\mathcal{N} = 4$ SYM compactified on a circle. At low energies this theory reduces to the three-dimensional gauge theory with confinement, mass gap and finite correlation length. The metric can be written as

$$ds^2 = \left(\frac{U}{L}\right)^2 \left[\left(\frac{L}{U}\right)^4 \frac{dU^2}{h(U)} + dx_\mu dx^\mu + h(U)dx_3^2\right] + L^2 d\Omega_5^2, \qquad \mu = 0, 1, 2 \tag{3.1}$$

where

$$h(U) = 1 - \left(\frac{U_0}{U}\right)^4, \qquad U_0^2 = \frac{L^4}{4R_3^2} \tag{3.2}$$

and R_3 is the radius of the Kaluza-Klein circle, and $L^4 = 4\pi\lambda = 4\pi g_s N_c$ sets the curvature scale of the AdS space.[3] It is convenient to switch to the variable $z = L^2/U$. The metric (3.1) takes the following form

$$ds^2 = L^2 \left[\frac{dz^2}{z^2 h(z)} + \frac{dx_\mu dx^\mu}{z^2} + h(z)\frac{dx_3^2}{z^2} + d\Omega_5^2\right] \tag{3.3}$$

where

$$h(z) = 1 - \frac{z^4}{z_0^4}, \qquad z_0 = 2R_3 \tag{3.4}$$

We follow [5], where the prescription to compute entanglement entropy was formulated in the holographic setup. Consider a disk in the $x_1 - x_2$ plane bounded by a circle of radius R, denoted by $\mathbf{S}^1_\phi$ below. The subscript here refers to the angular coordinate in the $x_1 - x_2$ plane; the radial coordinate is denoted by r. As reviewed in the previous section, the entanglement entropy for this disk can be computed by evaluating (2.3) on the minimal 8-dimensional surface at $t = const$ which asymptotes to $\mathbf{S}^1_\phi \times \mathbf{S}^1_{x^3} \times \mathbf{S}^5$ on the boundary at $z = 0$. In this computation we need to set $G_N^{(10)} = 8\pi^6 g_s^2$. The minimal surface is determined by specifying $z(r)$, with the induced metric $G^{(8)}_{\rm ind}$ given by

$$ds^2_{\rm ind} = L^2 \left[\frac{1}{z^2}\left(1 + \frac{(z')^2}{h(z)}\right) dr^2 + \frac{r^2}{z^2} d\phi^2 + \frac{h(z)}{z^2} dx_3^2 + d\Omega_5^2\right] \tag{3.5}$$

3.1 Conformal limit

We start with the warm-up example, which corresponds to the conformal theory, where the bulk geometry is $AdS_5 \times S^5$. In this limit $R_3 \to \infty$, $h(z) = 1$ and the region in the 3+1 dimensional boundary theory is the cylinder whose length we denote by l (of course, in the compactified case, $l = 2\pi R_3$). Eq. (2.3) can be written as

$$S = \frac{4N_c^2 l}{15\pi} \int dr \frac{r}{z^3} \sqrt{1 + (z')^2} \tag{3.6}$$

[3] Here and in the rest of the paper we set $\alpha' = 1$.

JHEP07(2008)097

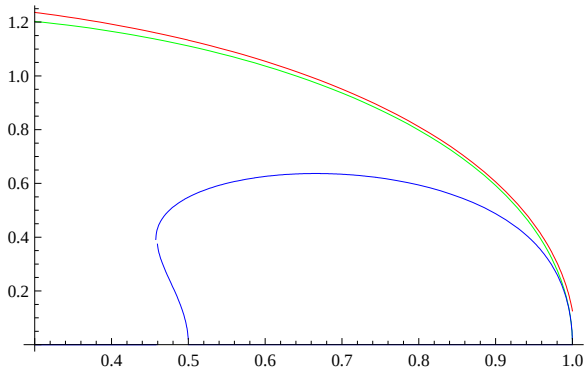

Figure 1: z(r) for $R = 0.5$, $\xi = 7 \times 10^{-7}$ and $R = 1$, $\xi = -6.1 \times 10^{-6}$ [blue curve]; $R = 1$, $\xi = -2 \times 10^{-6}$ [green curve] and $z(r = 0) = 1.29, z'(r = 0) = 0$ [red curve].

which gives the following equation of motion for the hypersurface:

$$\frac{d}{dr}\left(\frac{rz'}{z^3\sqrt{1+(z')^2}}\right) = -\frac{3r\sqrt{1+(z')^2}}{z^4} \tag{3.7}$$

One needs to specify the limits of integration in (3.6). For the hypersurface which asymptotes to the cylinder at $z = 0$ defined by $x_1^2 + x_2^2 < R^2$, the lower limit is $r = 0$ (we will elaborate on this in more detail below). Near the boundary the solution of interest behaves like $z(r) \to 0$ as $r \to R$ and the integral in (3.6) diverges near $r = R$ and needs to be regularized. We will introduce the upper limit of integration r_a by requiring that $z(r_a) = a$, where $a \to 0$ stands for short distance cutoff. In general, entanglement entropy is sensitive to the short-distant modes localized near the border of the region, and hence is cutoff-dependent. We will need to understand the behavior of $z(r)$ as $z \to 0$ (and $r \to R$). The leading term is easy to get from (3.7),

$$z \simeq 2\sqrt{R}\sqrt{R-r} \tag{3.8}$$

To go further in the expansion, it is convenient to introduce $x = 1 - R/r$ and make a substitution

$$z = 2R\sqrt{x}f(x) \tag{3.9}$$

which brings (3.7) into the form

$$\begin{aligned} 4x[x(1-x)f''(x) - 4x^2 f'(x)^3 + (4-5x)f'(x)]f(x) + f(x)^2[2-4x-24x^2 f'(x)^2] \\ +3(1-x)x(1+4xf'(x)^2) - 12xf(x)^3 f'(x) - 2f(x)^4 = 0 \end{aligned} \tag{3.10}$$

This equation has a solution in terms of the expansion

$$f(x) = 1 + a_1 x + a_2 x \log(x) + b_1 x^2 + b_2 x^2 \log(x) + b_3 x^2 \log(x)^2 + \dots \tag{3.11}$$

where $a_2 = 1/8$ and other coefficients determined by the value of a_1. Varying the value of a_1 we can vary the trajectory of the minimal surface in the AdS space. In practice, we

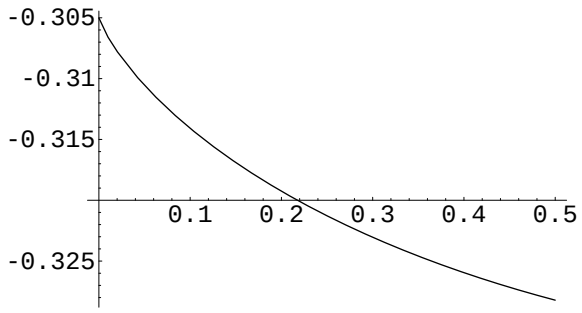

Figure 2: $-\widetilde{\gamma}$ as a function of $R - r_a$ for $R = 1$

specify initial conditions at the cutoff $z = a = 10^{-3}$ in the form

$$z(R) = a; \qquad z'(R) = -\frac{2R}{a}(1+\xi) \tag{3.12}$$

Varying ξ effectively varies the trajectory $z(r)$ originating at $z(R) = 0$. A generic trajectory looks like the blue curve in figure 1. It reaches a maximal value for z, then turns down and goes back to the boundary. The corresponding hypersurface asymptotes to two cylinders in the boundary theory. Some particular value of ξ corresponds to the surface which asymptotes to the cylinder of radius R at the boundary (this is the red curve in figure 1, it can also be obtained by requiring $z'(r = 0) = 0$). There are, of course, curves with smaller values of ξ. They look like the blue curve in figure 2, with the rescaled value of the radius, $r(z) \to 2r(z)$, and asymptote to two cylinders on the boundary.

In the following we will be interested in computing the value of entanglement entropy for the solution that asymptotes to the cylinder. It is a simple exercise to extract the UV-divergent term (see also [7]). For this purpose the parametrization $r(z)$ is more convenient. The value of expression (2.3) in this parametrization is

$$S = \frac{4N_c^2 l}{15\pi}\int_a dz \frac{r(z)}{z^3}\sqrt{1+\dot{r}^2} \tag{3.13}$$

where dot denotes derivative with respect to z and a is the UV cutoff. Inverting (3.9) and (3.11) we obtain

$$r = R\left[1 - \frac{z^2}{4R^2} + \mathcal{O}(z^4 \log z)\right] \tag{3.14}$$

this expression can be substituted into (3.13) to obtain

$$S = \frac{2N_c^2}{15\pi}\left(\frac{lR}{a^2} + \frac{l}{4R}\log\frac{a}{R}\right) - \frac{4N_c^2 l}{15\pi R}\widetilde{\gamma} \tag{3.15}$$

where $\widetilde{\gamma}$ is finite in the limit when short distance cutoff is taken to zero, $a \to 0$. Numerical evaluation of the integral (3.13) and subtraction of divergent terms in (3.15) produces a finite value of $\widetilde{\gamma} = 0.305$. In figure 2 we plot the (normalized) value of the integral in (3.6)

and observe that it is indeed finite in the limit $a \to 0$, $r_a \to R$. It is interesting that the limiting value of $\widetilde{\gamma}$ is positive and non-zero, similarly to the topological entropy in (2.6). Of course, in the conformal theory the correlation length is infinite, so it is not completely clear what the physical interpretation of nonvanishing $\widetilde{\gamma}$ is.

3.2 Finite compactification radius

Consider now the case with finite Kaluza-Klein radius R_3, and hence finite correlation length. For the rest of this section it will be convenient to pass to rescaled variables,

$$r \to \frac{r}{z_0}; \qquad z \to \frac{z}{z_0}; \qquad R \to \frac{R}{z_0} \tag{3.16}$$

It is useful to remember that $z_0 = 2R_3$ defines the scale of the correlation length in the theory. The rescaled coordinate z is now bounded from above by $z = 1$, where the Kaluza-Klein circle shrinks to zero size. Eq. (2.3) becomes

$$S = \frac{4N_c^2}{15} \int_0^{\frac{R}{z_0}} dr \frac{r}{z^3} \sqrt{1 - z^4 + (z')^2} \tag{3.17}$$

The equation of motion which follows from (3.17),

$$\frac{d}{dr}\left(\frac{rz'}{z^3\sqrt{1 - z^4 + (z')^2}} \right) = \frac{r(z^4 - 3[1 + (z')^2])}{z^4\sqrt{1 - z^4 + (z')^2}} \tag{3.18}$$

in general has to be solved numerically. A detailed study of possible solutions to (3.18) is relegated to the appendix. Here we briefly summarize the results. There are two types of solutions which asymptote to the circle of radius R in 2+1 dimensional boundary theory (they are shown in figure 3). One type involves a connected surface which approaches the circle of radius R near the boundary $z = 0$ and has the disk topology in the (r, ϕ) coordinates. It corresponds to the blue curve in figure 3. This solution can be found be starting at $r = 0$ with boundary conditions $z_* \equiv z(r = 0) < 1$, $z'(0) = 0$ and integrating (3.18) outwards in r. In figure 4 the value of R is plotted as a function of z_*. Similar to the slab geometry, studied in [15], there appears to be a maximal value of R, beyond which this solution does not exist. Moreover, in the first approximation there are two branches for sufficiently large values of R. The new feature in comparison with [15] is the existense of the lower bound on R for the branch which consists of the solutions passing close to the end of the space at $z = 1$. We will call the solution with $z_* \to 1$ critical, since, as we will see below, it joins with the solution which has the topology of the cylinder. (see below). We denote the value of R for such critical solution by R_c.

Another interesting solution, which was absent in the conformal case involves the surface which starts at $z = 1, r = r_0$ and goes all the way to the boundary. This surface has the topology of the cylinder in the (r, ϕ) coordinates and is an analog of the disconnected solution in [15]. It corresponds to the red curve in figure 3. To exhibit this solution (and for the purpose of computing the entanglement entropy below) it is convenient to use parametrization $r(z)$, like in (3.13). In the non-conformal case the action is given by

$$S = \frac{4N_c^2}{15\pi} \int_a dz \frac{r(z)}{z^3} \sqrt{1 + (1 - z^4)\dot{r}^2} \tag{3.19}$$

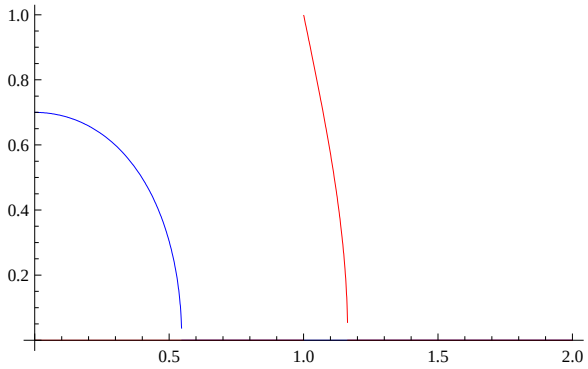

Figure 3: $z(r)$. Disk [blue] and cylinder [red] topology.

and the equation of motion

$$\frac{d}{dz}\frac{(1-z^4)r\dot{r}}{z^3\sqrt{1+(1-z^4)\dot{r}^2}} = \frac{\sqrt{1+(1-z^4)\dot{r}^2}}{z^3} \tag{3.20}$$

Near $z=1$ (3.20) has a solution

$$r = r_0 + \frac{1-z}{4r_0} + \dots \tag{3.21}$$

where r_0 is the value of r at $z=1$ and the dots stand for the terms subleading in $1-z$. Starting with these boundary conditions and integrating (3.20) or (3.18) numerically we obtain the solution with the topology of the cylinder. Note that at large r the solution of (3.21) can be found in the form

$$r = r_0 + \frac{f(z)}{r_0} + o(1/r_0) \tag{3.22}$$

We can also verify (3.22) numerically. In figure 5 we show the behavior of R as a function of r_0. At large r_0 we recover (3.22), but at small r_0 there is some interesting structure. As $r_0 \to 0$, the value of R approaches R_c and the solution approaches the critical solution (with the disk topology) discussed earlier. As r_0 increases, R goes down, before climbing up back again.

In addition to the two solutions described below, and just as in the conformal case studied above, there are also solutions which approach the two concentric circles on the boundary. Such solutions will define an annulus in the boundary 2+1 dimensional theory. We will not discuss them further; more details are provided in the appendix.

To compute the entanglement entropy we follow the steps of the previous subsection, where the conformal case was discussed. In particular, the divergent terms are again given by (3.15). We define the normalized finite part of the entropy $\widetilde{S}$ via

$$S = \frac{4N_c^2}{15}\left(\frac{RR_3}{a^2} + \frac{R_3}{4R}\log\frac{a}{R}\right) + \frac{4N_c^2}{15}\widetilde{S} \tag{3.23}$$

JHEP07(2008)097

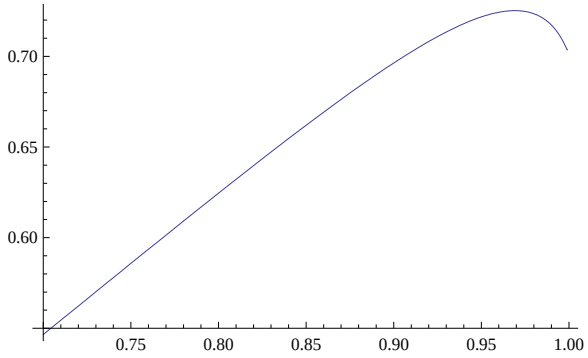

Figure 4: R as a function of z_* (solutions of disk topology)

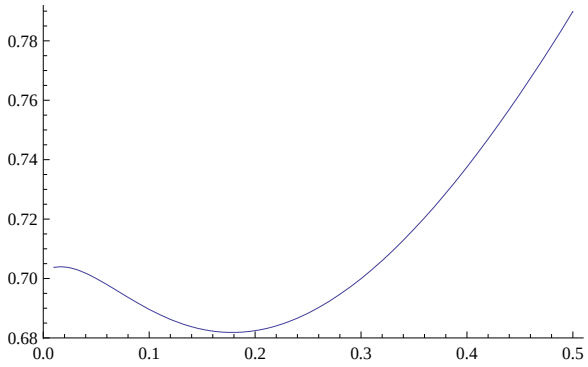

Figure 5: R as a function of r_0; (solutions of cylinder topology)

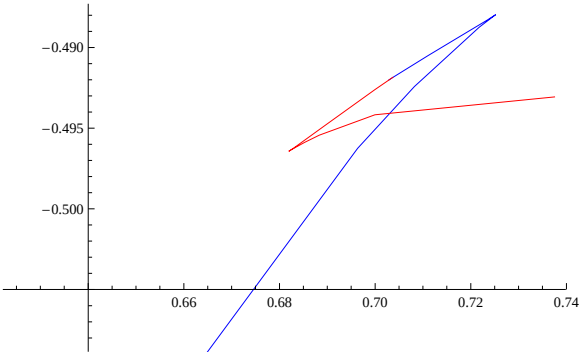

Figure 6: $\widetilde{S}$ as a function of R;

The value of $\widetilde{S}$ as a function of R [normalized according to (3.16)] is plotted in figure 6. The blue part of the curve corresponds to the solution which has the disk topology [blue curve in figure 3]. It is (modulo some fine details) double-valued, since R is a double-valued function of z_*, as can be inferred from figure 4. For a given value of R the branch with smaller z_* dominates the computation of entanglement entropy. The solution with $z_* \to 1$

JHEP07(2008)097

smoothly connects to the solution which has the topology of the cylinder (red curve in figures 3,6). The value of $\widetilde{S}$ for this solution is again double-valued, according to figure 5. As the value of R is increased, the cylinder solutions begins to dominate the entanglement entropy (this happens at the point where the red line crosses the blue in figure 6). For larger values of R only the solution with cylinder topology exists. According to (3.22), for large R,

$$r = R + \mathcal{O}(R^{-1}) \tag{3.24}$$

and hence

$$\widetilde{S} = -\frac{R}{2} + \mathcal{O}(R^{-1}) \tag{3.25}$$

which implies vanishing topological entropy γ.

4. D4 branes on a circle

In this section we will consider the entanglement entropy of a three-dimensional ball in a confining theory in $d = 3 + 1$. The theory is obtained from compactifying a $4 + 1$ theory with radius R_4 [16]. At strong coupling, it has a gravitational description with metric,

$$\begin{aligned} ds^2 &= \left(\frac{U}{R}\right)^{3/2}\left[\left(\frac{R}{U}\right)^3 \frac{dU^2}{f(U)} + dx_\mu dx^\mu + f(U)dx_4^2\right] + R^{3/2}U^{1/2}d\Omega_4^2, \qquad \mu = 0,1,2,3 \\ e^{-2\phi} &= \left(\frac{R}{U}\right)^{3/2} \end{aligned} \tag{4.1}$$

where $x_4 \sim x_4 + 2\pi R_4$ and

$$f(U) = 1 - \left(\frac{U_0}{U}\right)^3, \qquad U_0 = \frac{4\pi}{9}\frac{\lambda}{R_4^2} \tag{4.2}$$

The constant R is given by

$$R^3 = \pi\lambda, \tag{4.3}$$

where

$$\lambda \equiv (2\pi)^{-2} N_c g_{YM_5}^2 = g_s N_c l_s$$

is the five-dimensional 't Hooft coupling. The supergravity description is valid as long as $e^\phi \ll 1$,

$$U \ll R\,. \tag{4.4}$$

The boundary is at $U \to \infty$, and it is convenient to change the (U, x^μ) coordinates into $(z, \widetilde{x}^\mu)$ defined by

$$\begin{aligned} U &= \frac{U_0}{z} \\ x^\mu &= \left(\frac{R^3}{U_0}\right)^{1/2} \widetilde{x}^\mu \end{aligned} \tag{4.5}$$

We have now $z \in [0,1]$ and the boundary is at $z=0$. The metric and dilaton are now

$$\begin{aligned} ds^2 &= (R^3 U_0)^{1/2} \left\{ z^{-3/2} \left[\frac{dz^2}{z(1-z^3)} + d\widetilde{x}_\mu d\widetilde{x}^\mu + (1-z^3) d\widetilde{x}_4^2 \right] + z^{-1/2} d\Omega_4^2 \right\} \\ e^{-2\phi} &= \left(\frac{R}{U_0} \right)^{3/2} z^{3/2} \end{aligned} \tag{4.6}$$

We consider dividing the 3 spatial directions into a three-dimensional ball and its exterior, such that the surface between the two domains is a two-sphere. Therefore, we are interested in an 8-dimensional surface in the bulk, which wraps the inner 4-sphere, is constant along the periodic direction $\widetilde{x}^4$ and ends in a two-sphere of radius ρ in the boundary $z=0$.

Let us call r the radial coordinate in the $(\widetilde{x}^1, \widetilde{x}^2, \widetilde{x}^3)$ directions. The 8-dim surface is specified by the curve $z(r)$, or alternatively, by $r(z)$. Choosing z as the independent variable, the induced metric is

$$ds^2 = (R^3 U_0)^{1/2} \left\{ z^{-3/2} \left[\left(\frac{1}{z(1-z^3)} + \dot{r}^2(z) \right) dz^2 + r^2(z) d\Omega_2^2 + (1-z^3) d\widetilde{x}_4^2 \right] + z^{-1/2} d\Omega_4^2 \right\} \tag{4.7}$$

and the area functional (2.4) is

$$\begin{aligned} S &= \frac{1}{4 G_N^{(10)}} \int d^8\sigma e^{-2\phi} \sqrt{G_{\rm ind}^{(8)}} \\ &= \frac{\pi^3 R^6 U_0 R_4}{2 G_N^{(10)}} \int dz \, \frac{r^2(z)}{z^3} \sqrt{1 + z(1-z^3) r'^2(z)} \end{aligned} \tag{4.8}$$

where we have used $Vol(S^2) = \frac{4\pi}{3}$ and $Vol(S^4) = \frac{8\pi^2}{3}$. The equation of motion from this action is

$$\begin{aligned} &4 - 4z\left(-1+z^3\right) r'[z]^2 \\ &\quad + r[z] \left(2\left(2+z^3\right) r'[z] + z\left(5 - 7z^3 + 2z^6\right) r'[z]^3 + 2z\left(-1+z^3\right) r''[z] \right) = 0 \end{aligned} \tag{4.9}$$

Alternatively, choosing r as the independent variable, the induced metric and the area functional are

$$ds^2 = (R^3 U_0)^{1/2} \left\{ z^{-3/2} \left[\left(1 + \frac{z'^2(r)}{z(1-z^3)} \right) dr^2 + r^2 d\Omega_2^2 + (1-z^3) d\widetilde{x}_4^2 \right] + z^{-1/2} d\Omega_4^2 \right\} \tag{4.10}$$

$$S = \frac{\pi^3 R^6 U_0 R_4}{2 G_N^{(10)}} \int dr \, \frac{r^2}{z^3(r)} \sqrt{z(r)(1-z^3(r)) + z'^2(r)} \tag{4.11}$$

and the equations of motion are

$$\begin{aligned} &2rz[r]^7 + 2rz[r]^3 z'[r]^2 + 4z'[r]^2 \left(r + z'[r]\right) \\ &\qquad + z[r]\left(4z'[r] + r\left(5 + 2z''[r]\right)\right) - z[r]^4 \left(4z'[r] + r\left(7 + 2z''[r]\right)\right) = 0 \end{aligned} \tag{4.12}$$

4.1 The two topologies

The shape of the surfaces we are looking for is determined by the functions $r(z)$ or $z(r)$. As in the previous section, starting with $z = 0$ at $r = \rho$, there are two possible shapes for $z(r)$:

1) the curve starts from $z = 0$ at $r = \rho$ and reaches $z = 1$ at some value $r = r_0$. We call these curves of 'cylinder' topology.

2) the curve starts from $z = 0$ at $r = \rho$ and ends at $r = 0$ with $z = z_0 \leq 1$. To avoid a conical singularity, we should demand $z'(0) = 0$. We call these curves of 'disk' topology.

In practice we can obtain the curves numerically. For the disk topology, the initial conditions of the numerical problem are $z(0) = z_0$, $z'(0) = 0$.[4]

For the cylinder topology, the numerical problem can be set to find either $z(r)$ or $r(z)$, and in both cases we can set the boundary conditions either at $z = 0$ or at $z = 1$. Consider the latter case first. With the boundary condition $z(r_0) = 1$, the leading term in the solution of (4.12) is

$$z(r) \simeq 1 - \frac{3}{2} r_0 (r - r_0) \tag{4.13}$$

One can check that inverting this function,

$$r(z) \simeq r_0 + \frac{2}{3 r_0} (1 - z)\,, \tag{4.14}$$

gives the leading term of the solution of (4.9) with b.c. $r(1) = r_0$. From the expressions (4.13) or (4.14) one can read out the boundary values of $z'(r_0)$ or $r'(1)$ needed for the numerical solution.

Alternatively, we can consider the behavior of the solutions near $z = 0$. The leading term in the solution of eq. (4.12) near the boundary ($z \sim 0$), with boundary condition $z(\rho) = 0$, is[5]

$$z(r) \simeq \rho(\rho - r) + \cdots \tag{4.15}$$

The inverse to the above function has the expansion

$$r(z) \simeq \rho - \frac{z}{\rho} - \frac{3 z^2}{4 \rho^3} + \cdots \tag{4.16}$$

which are the leading terms of the solution of (4.9) with b.c. $r(0) = \rho$. One can verify that the series (4.16) contains terms of the type $z^n \ln^m z$, starting with $z^4 \ln z$. From the expressions (4.15) or (4.16) one can read the boundary values of $z'(\rho)$ or $r'(0)$ which can be used in the numerical solutions.

In figure 7 we show the profile of $z(r)$ for solutions of both topologies. As z_0 approaches 1, there is a smooth transition between the two topologies, since the 'disk' solution with $z_0 = 1$ coincides with the 'cylinder' solution with $r_0 = 0$.

The value of $r(0) = \rho$ has an interesting dependance on the value of z_0 and r_0 for the 'cylinder' and 'disk' solutions, respectively, as we show in figures 8 and 9.

[4] One can also try to find numerically the 'disk' solutions by fixing the boundary conditions at $z = 0$

JHEP07(2008)097

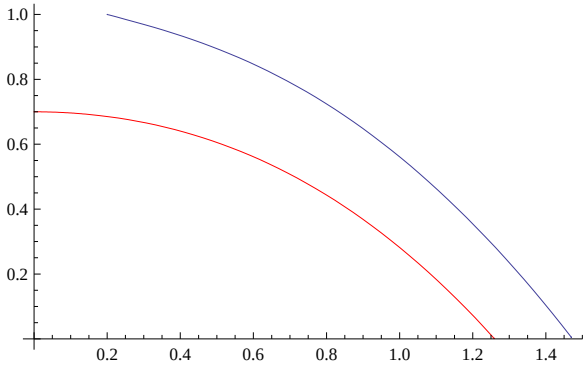

Figure 7: Shape of $z(r)$ for a 'cylinder' solution with $r_0 = 0.2$ [blue] and for a 'disk' solution with $z_0 = 0.7$ [red].

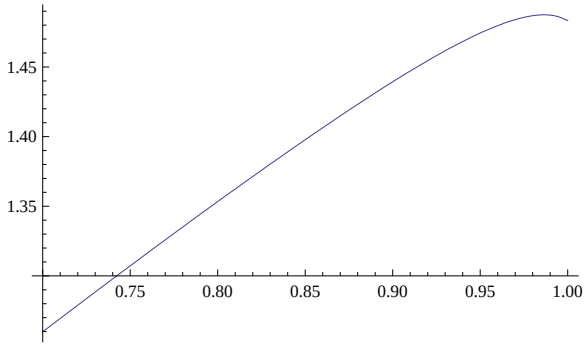

Figure 8: ρ as function of z_0 for the 'disk' solutions.

We see that for the 'disk' solutions there is a maximal value ρ as z_0 grows, and for bigger z_0 the value of ρ shrinks. A more detailed numerical study, which is not evident in figure 8, shows that the value of ρ actually oscillates with decreasing amplitude as $z_0 \to 1$. For the 'cylinder' solutions, ρ grows monotonically with r_0 for large r_0. As r_0 diminishes, there is a minimum value for ρ, such that for smaller values of r_0, ρ starts to grow again. Also here a close look shows that the value of ρ oscillates with decreasing amplitude as $r_0 \to 0$.

4.2 The phase transition

The entanglement entropy is UV-divergent and we will be interested in subtracting the divergencies and obtaining a finite quantity. The divergent terms in the entanglement

(instead of at $r = 0$), but the shape of the curve is very sensitive to the initial conditions and a slightly bigger or smaller value for $z'(\rho)$ does not give a solution ending at $r = 0$ with $z'(0) = 0$.

[5]There is a second solution to (4.12) that behaves as $z(r) \simeq -\frac{1}{4}(\rho - r)^2$, but it is not physical since $z \in [0, 1]$.

JHEP07(2008)097

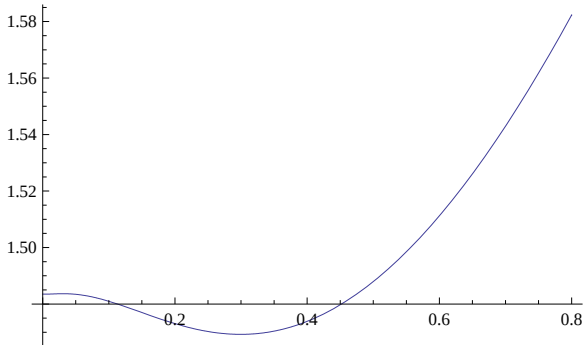

Figure 9: ρ as a function of r_0 for the 'cylinder' solutions.

entropy can be obtained by inserting the leading behavior (4.16) into (4.8). This gives

$$\begin{aligned} S &= \frac{\pi^3 R^6 U_0 R_4}{2G_N^{(10)}} \int_a^1 dz \, \frac{r^2(z)}{z^3} \sqrt{1 + z(1-z^3) r'^2(z)} \\ &= \frac{\pi^3 R^6 U_0 R_4}{2G_N^{(10)}} \left[\frac{\rho^2}{2a^2} - \frac{3}{2a} + \frac{\ln a}{8\rho^2} \right] + S_{\text{finite}}(a) \end{aligned} \tag{4.17}$$

where $S_{\text{finite}}(a)$ is finite as $a \to 0$.[6] Unlike the slab geometry, the divergent term does depend on the size ρ. In figure 10 we show the value $S_{\text{finite}}(0)$ as a function of ρ. Note that this is a multivalued function, since a given ρ can correspond to two different values of z_0 or r_0, as we saw above.

4.3 Topological entropy

To compute the topological entropy only the cylinder solutions are relevant, since we are interested in the the limit $\rho \to \infty$. For the same reason, it is convenient to expand the solution in powers of ρ as

$$r(z) = \rho + f(z) + \frac{g(z)}{\rho} + \frac{h(z)}{\rho^2} + \cdots \tag{4.18}$$

where $f(0) = g(0) = h(0) = \ldots = 0$. Inserting this expansion in the equation of motion (4.9) for $r(z)$, gives for the leading term ($\sim \rho$),

$$4f'[z] + 2z^3 f'[z] + 5z f'[z]^3 - 7z^4 f'[z]^3 + 2z^7 f'[z]^3 - 2z f''[z] + 2z^4 f''[z] = 0 \tag{4.19}$$

This equation is solved by $f'(z) = 0$, and from $f(0) = 0$ we get that $f(z) = 0$. With this result, the next term in the equation of motion (4.9) for $r(z)$ ($\sim \rho^0$) is

$$4 + 4g'[z] + 2z^3 g'[z] - 2z g''[z] + 2z^4 g''[z] = 0 \tag{4.20}$$

[6] It is interesting that from the r^2 and r'^2 dependence in (4.17) there are contributions from the z^2 term in (4.16) to the $\ln a$ term in (4.17), but one can check that they cancel and the divergence would be the same had we kept only the linear term in (4.16).

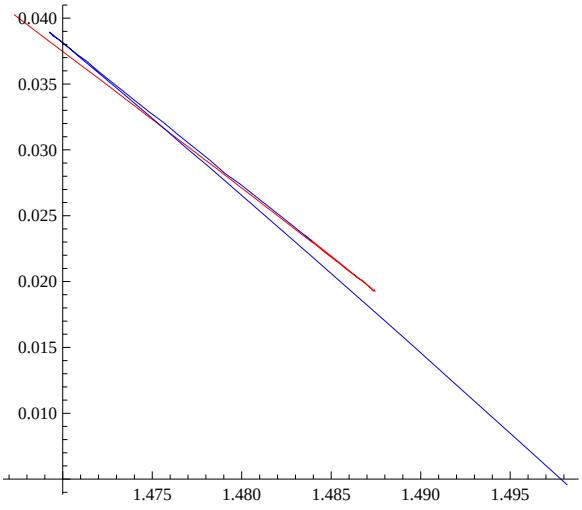

Figure 10: The finite entanglement entropy $S_{\text{finite}}(0)$ as a function of ρ. The red line corresponds to the 'disk' topology and the blue line to the 'cylinder' topology.

which has the exact solution

$$g'(z) = -\frac{1+cz^2}{1-z^3}\,, \tag{4.21}$$

and c is an integration constant. The 'cylinder' solutions are required to be regular at $z=1$, and this fixes $c=-1$, so we have

$$g'(z) = -\frac{1+z}{1+z+z^2} \tag{4.22}$$

Integrating this function gives

$$\begin{aligned} g(z) &= -\frac{\arctan\left[\frac{1+2z}{\sqrt{3}}\right]}{\sqrt{3}} - \frac{1}{2}\log\left[1+z+z^2\right] + \frac{\pi}{6\sqrt{3}} \\ &= -\left(z+\frac{z^4}{4}+\frac{z^7}{7}+\cdots\right)+\left(\frac{z^3}{3}+\frac{z^6}{6}+\frac{z^9}{9}+\cdots\right), \end{aligned} \tag{4.23}$$

where the integration constant is fixed by $g(0)=0$.

As it turns out, the 'topological' term in the entanglement entropy depends only on $g(z)$ and therefore can be computed exactly. Indeed, inserting the expansion (4.18) into (4.8) gives, using $f(0)=0$,

$$\begin{aligned} S &= \frac{\pi^3 R^6 U_0 R_4}{2G_N^{(10)}}\int_a^1 dz\left[\frac{\rho^2}{z^3}+\frac{4g[z]+z\left(1-z^3\right)g'[z]^2}{2z^3}\right]+O(\rho^{-1}) \\ &= S_{\rho^2}-\gamma+O(\rho^{-1}) \end{aligned} \tag{4.24}$$

where

$$\begin{aligned} S_{\rho^2} &= \frac{\pi^3 R^6 U_0 R_4}{4G_N^{(10)}} \rho^2 \left(\frac{1}{a^2} - 1\right) \\ &= \frac{\pi^3 R^3 R_4 r_m^2}{4G_N^{(10)}} \left(U_\infty^2 - U_0^2\right) \\ \gamma &= -\frac{\pi^3 R^6 U_0 R_4}{8G_N^{(10)}} \left(\frac{\pi}{3} + 2 + \log 3 - \frac{6}{a}\right) \\ &= -\frac{\pi^3 R^6 U_0 R_4}{8G_N^{(10)}} \left(\frac{\pi}{3} + 2 + \log 3 - \frac{6U_\infty}{U_0}\right) \end{aligned} \tag{4.25}$$

where $U_\infty = U_0/a$, and the dimensionful radius of the ball is $r_m^2 = \rho^2 R^3/U_0$. In order to express the entropy using gauge theory quantities we should use

$$G_N^{(10)} = 8\pi^6 g_s^2 = \frac{8\pi^6 \lambda^2}{N_c^2} \tag{4.26}$$

and the relation between U_∞ and the field theory cutoff Λ in our background [28],

$$U_\infty = g_{YM_5}^2 N_c \Lambda^2 = (2\pi)^2 \lambda \Lambda^2 \tag{4.27}$$

This gives finally

$$\begin{aligned} S_{\rho^2} &= \lambda N_c^2 r_m^2 R_4 \left(\frac{\pi^2 \Lambda^4}{2} - \frac{1}{3^4 R_4^4}\right) \\ \gamma &= -\frac{\lambda N_c^2}{144 R_4} \left(\frac{\pi}{3} + 2 + \log 3 - 9\pi \Lambda^2 R_4^2\right) \end{aligned} \tag{4.28}$$

So we find a non-zero and cutoff dependent topological entanglement entropy. But we should remember that the supergravity description can only be trusted in the limit (4.4), which for the cutoff Λ means,

$$\Lambda \ll \frac{1}{(\lambda \alpha')^{1/3}} \,. \tag{4.29}$$

5. Discussion

In this paper we computed the entanglement entropy for a disk in 2+1 dimensions and a ball in 3+1 dimensions in the confining theories with holographic duals. We observed a phase structure similar to the one found in [15], with two types of solutions. At small values of R the solution of the disk topology dominates the computation of entanglement entropy, while at large values of R the cylinder type solution dominates. In 2+1 dimensions this structure ensures vanishing topological entropy, which is an expected result for a QCD-type theory. This can also be viewed as a consistency check of the holographic prescription. (Of course, it would be great to make progress in understanding the prescription of Takayanagi and Ryu from the first principles.) It is interesting that in the conformal case the analog of the topological entropy is nonzero. It is not completely clear what the physical interpretation of this fact is.

JHEP07(2008)097

In 3+1 dimensions one can define a quantity which is analogous to topological entropy. It turns out to be UV divergent. A possible explanation of this behavior is that, as mentioned, the supergravity description of the field theory cannot be trusted beyond the bound (4.29). On the other hand, the topological entropy has not been studied much in 3+1 dimensions, and such studies might shed light on our result.

Both in the 2+1 and 3+1 cases the solution with the disk topology joins the solution with the cylinder topology at some critical value of the disk or ball radius. The behavior of the entanglement entropy near this point seems reminiscent of self-similar type of behavior of free energy of probe branes, described in [29]. It would be interesting to investigate this in more detail.

For the slab geometry, signatures of the phase transition predicted in [15] have recently been found in numerical studies in the lattice [30] (see also [31]). It would be interesting to seek for similar signatures of the phase transition predicted by the disk and spherical geometries. But it should be noted that, unlike the case of the slab geometry [15], in our case the (regularized) entropy scales as N_c^2 at both sides of the critical point. This suggests that the existence of the phase transition might be unrelated to the confining properties of the theory. Studying entanglement entropy for other geometries, different from disks and slabs, might also shed light on the relation of entanglement entropy to the properties of the theory.

Finally, it would be interesting to find supergravity backgrounds which would correspond to theories with non-zero topological entanglement entropy. One instance could be the system of D2-D6 branes which models the Quantum Hall effect [32], but to apply the methods of this paper one would need the full supergravity solution, and not only the probe approximation used in [32].

Acknowledgments

We thank S. Giombi, C. Herzog, I. Klich, M. Levin, M. Kulaxizi and D. Kutasov for discussions. Ari Pakman thanks Harvard University for hospitality. The work of Ari Pakman is supported by the Simons Foundation. Andrei Parnachev thanks KITP, Santa Barbara, University of Amsterdam, Ecole Polytechnique and University of Washington for hospitality during the course of this work.

A. Solutions in detail

To investigate the structure of the solutions of (3.18) and (3.20) we repeat the analysis of section 3.1. The UV behavior of the solution of (3.18) still satisfies (3.9) and (3.11), although eq. (3.10) is modified. Typical behavior of the solutions for sufficiently small R are shown in figure 11. The picture is completely similar to the one in figure 1, which is not surprising, since R is substantially smaller than the correlation length. In figure 12 $r(z)$ is computed. In particular, there is a maximal value of z which the curves can attain. The red and blue curves in figure 12 approximate to the annuli with internal radius $R_i = R = 0.468$ and external radius $R_e > R$. The green curve in figure 12. (which is the

JHEP07(2008)097

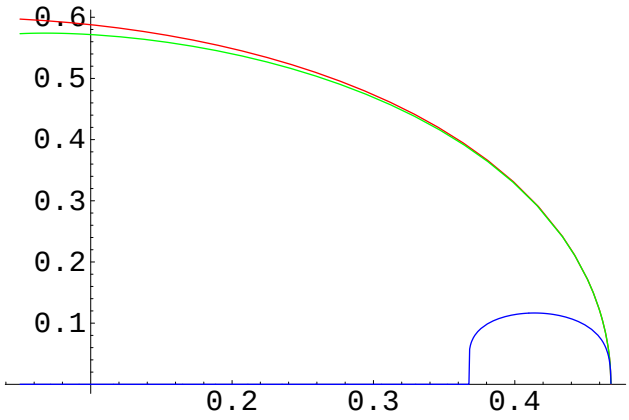

Figure 11: $z(r)$ in confining background for $R = 0.468$; $\xi = -5 \times 10^{-4}$ [blue curve]; $\xi = -8.05 \times 10^{-6}$ [green curve]; $z'(r = 0) = 0$ [red curve]

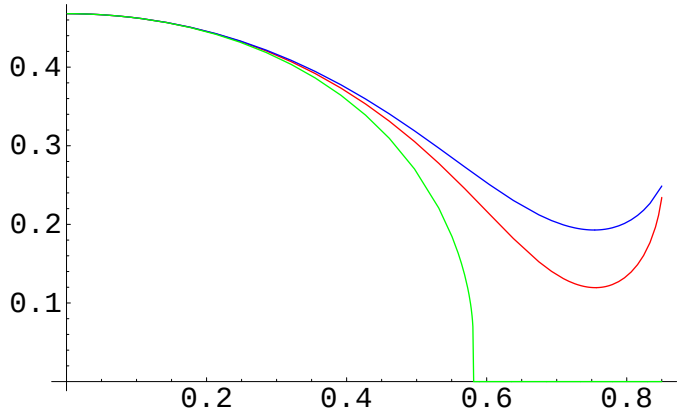

Figure 12: $r(z)$ in confining background for $R = 0.468$;

counterpart of the green curve in figure 11) gets very close to the connected solution but eventually approximates to the annuli with $R_e = R = 0.468$, $R_i \ll R$. In figure 13 we plot the structure of the solutions for the critical value of $R = R_c = 0.7034$. The blue curve is essentially the critical solution, while the red curve comes very close to $z = z_0$ before turning up and ending back on the boundary again. It is instructive to see how this picture changes for $R > R_c$ in figure 14. We now start with $R = 1 > R_c$. The red line gives rise to the annulus with $R_i < R_e = 1$, while the blue line corresponds to $R_e > R_i = 1$ and comes very close to $z = z_0$. The green line separates the two domains; it is natural to think that it ends at $z = z_0$ and gives rise to a surface with annulus topology in the bulk (not to be confused with the topology of the boundary which is a circle). This is the analog of the disconnected solution in [15]. This solution can be exhibited in a more direct way. One can analyze the equation of motion near $z = 1, r = r_0 > 0$ and integrate the solution from there. This is done in section 3.2.

JHEP07(2008)097

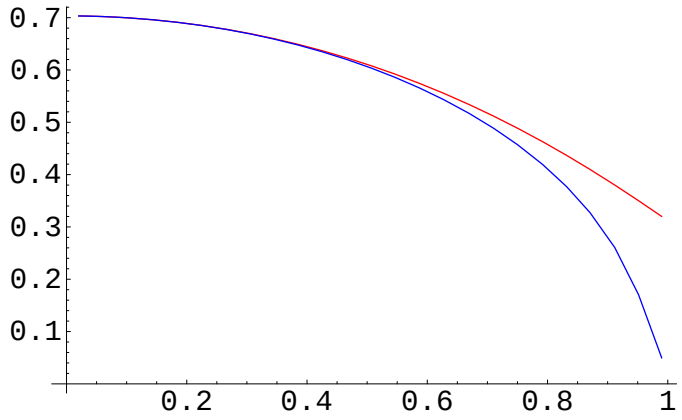

Figure 13: $r(z)$ in confining background for $R = R_c = 0.7034$;

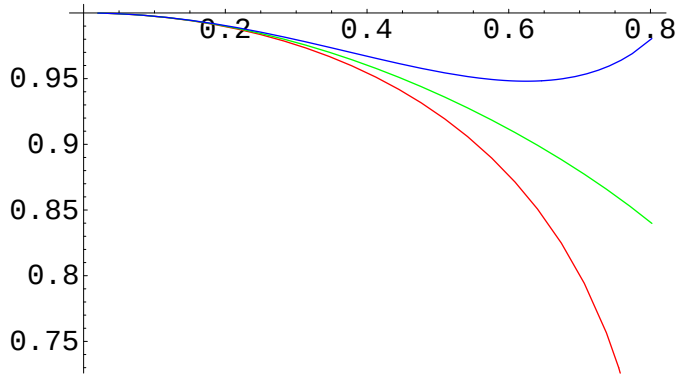

Figure 14: $r(z)$ in confining background for $R = 1 > R_c$;

References

[1] X.G. Wen and Q. Niu, *Ground state degeneracy of the FQH states in presence of random potential and on high genus Riemann surfaces*, *Phys. Rev.* **B41** (1990) 937.

[2] X.G. Wen, *Topological orders and edge excitations in FQH states*, *Adv. in Phys.* **44** (1995) 405.

[3] A. Kitaev and J. Preskill, *Topological entanglement entropy*, *Phys. Rev. Lett.* **96** (2006) 110404 [hep-th/0510092].

[4] M. Levin and X.-G. Wen, *Detecting topological order in a ground state wave function*, *Phys. Rev. Lett.* **96** (2006) 110405.

[5] S. Ryu and T. Takayanagi, *Holographic derivation of entanglement entropy from AdS/CFT*, *Phys. Rev. Lett.* **96** (2006) 181602 [hep-th/0603001]; *Aspects of holographic entanglement entropy*, *JHEP* **08** (2006) 045 [hep-th/0605073].

[6] A. Schwimmer and S. Theisen, *Entanglement entropy, trace anomalies and holography*, *Nucl. Phys.* **B 801** (2008) 1 [arXiv:0802.1017].

JHEP07(2008)097

[7] S.N. Solodukhin, *Entanglement entropy, conformal invariance and extrinsic geometry*, arXiv:0802.3117.

[8] T. Hirata and T. Takayanagi, *AdS/CFT and strong subadditivity of entanglement entropy*, *JHEP* **02** (2007) 042 [hep-th/0608213].

[9] M. Headrick and T. Takayanagi, *A holographic proof of the strong subadditivity of entanglement entropy*, *Phys. Rev.* **D 76** (2007) 106013 [arXiv:0704.3719].

[10] V.E. Hubeny, M. Rangamani and T. Takayanagi, *A covariant holographic entanglement entropy proposal*, *JHEP* **07** (2007) 062 [arXiv:0705.0016].

[11] J.L.F. Barbon and C.A. Fuertes, *Holographic entanglement entropy probes (non)locality*, *JHEP* **04** (2008) 096 [arXiv:0803.1928].

[12] D.V. Fursaev, *Proof of the holographic formula for entanglement entropy*, *JHEP* **09** (2006) 018 [hep-th/0606184].

[13] T. Nishioka and T. Takayanagi, *AdS bubbles, entropy and closed string tachyons*, *JHEP* **01** (2007) 090 [hep-th/0611035].

[14] J.L.F. Barbon and C.A. Fuertes, *A note on the extensivity of the holographic entanglement entropy*, *JHEP* **05** (2008) 053 [arXiv:0801.2153].

[15] I.R. Klebanov, D. Kutasov and A. Murugan, *Entanglement as a probe of confinement*, *Nucl. Phys.* **B 796** (2008) 274 [arXiv:0709.2140].

[16] E. Witten, *Anti-de Sitter space, thermal phase transition and confinement in gauge theories*, *Adv. Theor. Math. Phys.* **2** (1998) 505 [hep-th/9803131].

[17] L. Bombelli, R.K. Koul, J.-H. Lee and R.D. Sorkin, *A quantum source of entropy for black holes*, *Phys. Rev.* **D 34** (1986) 373.

[18] M. Srednicki, *Entropy and area*, *Phys. Rev. Lett.* **71** (1993) 666 [hep-th/9303048].

[19] J.M. Maldacena, *The large-N limit of superconformal field theories and supergravity*, *Adv. Theor. Math. Phys.* **2** (1998) 231 [*Int. J. Theor. Phys.* **38** (1999) 1113] [hep-th/9711200];
S.S. Gubser, I.R. Klebanov and A.M. Polyakov, *Gauge theory correlators from non-critical string theory*, *Phys. Lett.* **B 428** (1998) 105 [hep-th/9802109];
E. Witten, *Anti-de Sitter space and holography*, *Adv. Theor. Math. Phys.* **2** (1998) 253 [hep-th/9802150].

[20] D.C. Tsui, H.L. Stormer and A.C. Gossard, *Two-dimensional magnetotransport in the extreme quantum limit*, *Phys. Rev. Lett.* **48** (1982) 1559.

[21] X.G. Wen, *Topological order in rigid states*, *Int. J. Mod. Phys.* **B 4** (1990) 239.

[22] X.G. Wen, *Vacuum degeneracy of chiral spin states in compactified space*, *Phys. Rev.* **B40** (1989) 7387.

[23] D. Arovas, J.R. Schrieffer and F. Wilczek, *Fractional statistics and the quantum Hall effect*, *Phys. Rev. Lett.* **53** (1984) 722.

[24] C. Nayak and F. Wilczek, $2n$ *quasihole states realize* 2^{n-1}*-dimensional spinor braiding statistics in paired quantum Hall states*, *Nucl. Phys.* **B479** (1996) 529 [cond-mat/9605145];
N. Read and E. Rezayi, *Quasiholes and fermionic zero modes of paired fractional quantum hall states: the mechanism for non-abelian statistics*, *Phys. Rev.* **B54** (1996) 16864 [cond-mat/9609079].

JHEP07(2008)097

[25] P. Fendley, M.P.A. Fisher and C. Nayak, *Topological entanglement entropy from the holographic partition function*, *J. Statist. Phys.* **126** (2007) 1111 [cond-mat/0609072].

[26] S. Dong, E. Fradkin, R.G. Leigh and S. Nowling, *Topological entanglement entropy in Chern-Simons theories and quantum Hall fluids*, *JHEP* **05** (2008) 016 [arXiv:0802.3231];

[27] A. Hamma, P. Zanardi and X.G. Wen, *String and membrane condensation on 3D lattices*, *Phys. Rev.* **B 72** (2005) 035307 [cond-mat/0411752];
H. Bombin and M.A. Martin-Delgado, *Exact topological quantum order in $D = 3$ and beyond: branyons and brane-net condensates*, *Phys. Rev.* **B 75** (2007) 075103 [cond-mat/0607736].

[28] A.W. Peet and J. Polchinski, *UV/IR relations in AdS dynamics*, *Phys. Rev.* **D 59** (1999) 065011 [hep-th/9809022].

[29] D. Mateos, R.C. Myers and R.M. Thomson, *Holographic phase transitions with fundamental matter*, *Phys. Rev. Lett.* **97** (2006) 091601 [hep-th/0605046].

[30] P.V. Buividovich and M.I. Polikarpov, *Numerical study of entanglement entropy in* SU(2) *lattice gauge theory*, arXiv:0802.4247.

[31] A. Velytsky, *Entanglement entropy in $d + 1$ SU(N) gauge theory*, *Phys. Rev.* **D 77** (2008) 085021 [arXiv:0801.4111].

[32] J.H. Brodie, L. Susskind and N. Toumbas, *How Bob Laughlin tamed the giant graviton from Taub-NUT space*, *JHEP* **02** (2001) 003 [hep-th/0010105];
S.S. Gubser and M. Rangamani, *D-brane dynamics and the quantum Hall effect*, *JHEP* **05** (2001) 041 [hep-th/0012155].

JHEP07(2008)097